Development of a cascaded controller for temperature and core growth rate in vapour-phase axial deposition

H E Jenkins[1]* and **M L Nagurka**[2]
[1]Department of Mechanical Engineering, Mercer University, Macon, Georgia, USA
[2]Department of Mechanical Engineering, Marquette University, Milwaukee, Wisconsin, USA

The manuscript was received on 22 January 2009 and was accepted after revision for publication on 7 May 2009.

DOI: 10.1243/09596518JSCE743

Abstract: A cascaded feedback control strategy for an industrial vapour-phase axial deposition (VAD) process is investigated in this paper. VAD is a widely used process in the creation of high-purity glass for optical fibre. In previous work a soot tip surface temperature controller was developed for the VAD process to reduce the effects of core soot temperature variation on deposition geometry, leading to a more stable process. However, it is desired to regulate both the core soot and clad soot such that they deposit at the same axial rate to provide a more uniform product. This paper presents the development of a cascaded controller strategy and process model to couple and regulate the surface temperature and deposition rates of core and clad soot. Simulation studies demonstrate a potential improvement in the uniformity of the core and clad soot geometry over the soot product length.

Keywords: optical fibre fabrication, process control, VAD

1 INTRODUCTION

This paper proposes a cascaded control method for vapour-phase axial deposition (VAD), a commonly used multistep process for the manufacture of high-quality glass for optical fibre. The process deposits a glass soot mixture of silicon dioxide and germanium dioxide to create the light guide core and cladding around the core. It is desirable to maintain consistent core and clad geometry throughout the manufacturing process to create a high-performance optical fibre product for high bandwidth data transmission. Common practice in the VAD process is for the core and clad soot deposition rates, as well as the related surface temperature, to run essentially open-loop while regulating constant flowrates of gases and chemicals to the deposition torches. This situation yields varying diameters of core and clad soot regions reducing the usable length of the final glass and lowering product yield.

*Corresponding author: Department of Mechanical Engineering, Mercer University, 1400 Coleman Avenue, Macon, GA 30253, USA.
email: jenkins_he@mercer.edu

The VAD process was invented at NTT Laboratories in Japan and is the dominant production method for Japanese manufacturers of optical fibre. VAD is an improvement of the Corning OVD (outside vapour deposition) process [**1**, **2**]. The VAD process has been the subject of previous studies [**3**–**5**]. However, developments in modelling and control of the process are still actively pursued in industry [**6**].

This work focuses on the glass soot creation step in the VAD process. Soot making and deposition are typically accomplished via two torches in a vertical process chamber with a rotating chuck, as shown in Fig. 1. A core torch creates circular inner core soot from a mixture of germanium dioxide, silicon dioxide, oxygen, and fuel (typically hydrogen). A pure silicon dioxide soot layer is concurrently deposited from a second (clad) torch, as part of the final cladding around the core. The germanium dioxide component of the core region increases the refractive index of the light guide core over the index of the surrounding cladding glass in the resulting optical fibre. (Basic glass chemistry and flame hydrolysis reactions for the glass process in VAD are reviewed in several references [**3**, **4**, **7**].)

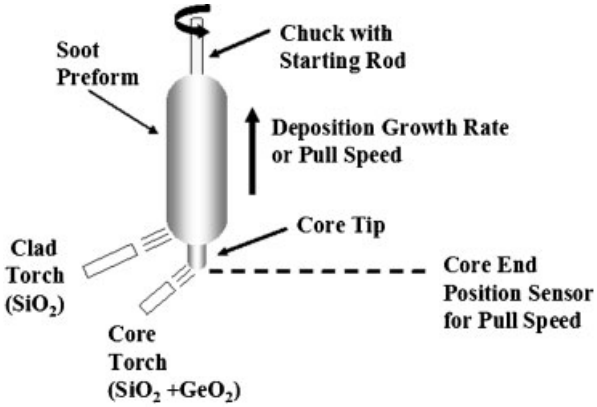

Fig. 1 VAD process depicting core and clad torches depositing glass soot onto the rotating preform. The core tip position is held constant, causing the preform and chuck to move upward

The rotating chuck moves upwards as glass soot is deposited to form a 'preform'. The preform moves upwards by a position control loop that uses laser light to indicate the core tip position. As the soot core tip grows from deposited soot, it blocks the light signal, causing the servo stage to move upwards. This upward movement of the preform is commonly referred to as the pull speed. The pull speed is a result of position control to keep the bottom of the core tip in the same location as the soot preform grows. Thus, the pull speed is the core soot deposition axial growth rate. In contrast, the cladding growth is not controlled. After the soot preform has reached the design length (1 m or larger), a sequential sintering operation is used to consolidate the glass soot into a solid glass preform. It is then nearly ready to draw into optical fibre.

2 PROBLEM DESCRIPTION

2.1 VAD processing background

Common practice in VAD processing is for the core and clad soot deposition rates, as well as the related surface temperatures, to run essentially open-loop. Each deposition torch (core and clad) has regulated flowrates of chemicals and gases (determined *a priori* by trial and error). Although the goal is to match perfectly the deposition rates of the clad and core torches, it is rarely accomplished. The core region may grow faster than the clad, or vice versa. In addition, the soot preform core tip length may grow or shrink relative to the cladding, making the diameter ratios of the clad to core (D/d) vary. This D/d variation results in a less uniform product, requiring additional processing and increasing waste. These diameters and variations can be visualized in Fig. 2. Final soot preforms show open-loop process variation as indicated by the non-uniform or tapering outside diameters (D) or varying-length core tips.

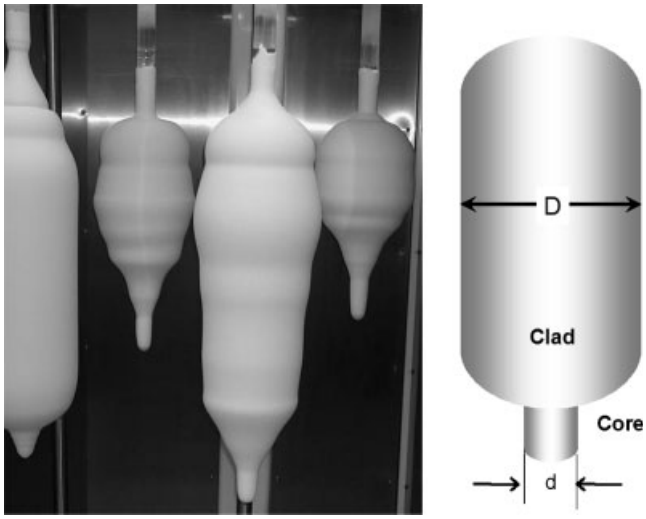

Fig. 2 Variation in soot outside diameters and core tip length (core tip diameters depicted are nominally 40 mm)

Length changes of the core tip with time indicate that the core and clad torch deposition rates are mismatched. Keeping the core tip length constant will be the goal of the process control strategy developed in this paper. Proper control will force soot growth rates for the core and clad to be matched and will also result in a constant D/d ratio. As depicted in Fig. 3, the core tip length (L_{CORE}) can be determined by the time integral of the deposition

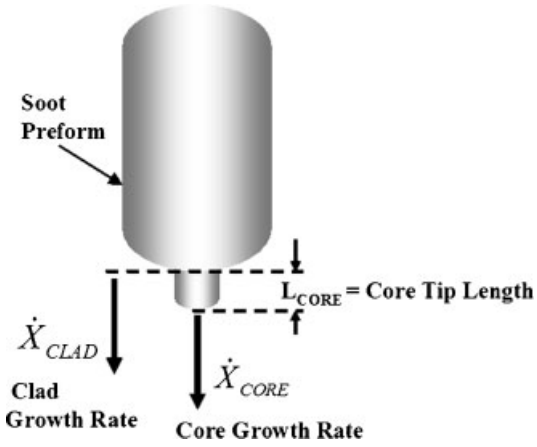

Fig. 3 Core and clad growth rates for soot preform creation

growth rates of the core and clad sections of the soot preform, $\dot{X}_{\mathrm{CORE}}$ and $\dot{X}_{\mathrm{CLAD}}$ respectively, as given by

$$L_{\mathrm{CORE}} = L_{\mathrm{o}} + \int \dot{X}_{\mathrm{CORE}} \mathrm{d}t - \int \dot{X}_{\mathrm{CLAD}} \mathrm{d}t \tag{1}$$

The core soot substrate tip temperature can be used to control the core deposition rate (pull speed) and ultimately the core tip length (between the core and clad deposition surfaces). In previous work, the core deposition rate was shown to be controllable by the H_2 flow to the core torch [**8**]. Therefore, control of the core tip length may be accomplished by slowing or increasing the rate of the core deposition, $\dot{X}_{\mathrm{CORE}}$, while leaving the clad deposition rate constant.

In earlier work a soot tip surface temperature controller was developed for the VAD process to reduce the effects of core soot temperature variation on deposition, leading to a more stable process [**8**]. However, this approach did not address the need to regulate and link the deposition rates of the core and clad torches. If the core soot and clad soot deposit at the same axial growth rate (pull speed) such that the core and clad deposition surfaces maintain a constant distance between each other, a more uniform product will result.

Presented in this paper is the development of a controller to couple and regulate the core surface temperature and the resulting core soot deposition rate. Simulation studies of the process control demonstrate a potential improvement in the uniformity of the core and clad soot geometry over the preform length. It is noted that the clad deposition rate can be measured by a variety of available low-cost devices, including optical phototransistors or machine vision.

2.2 Soot deposition process characteristics

The presented crystalline structure for the GeO_2 and SiO_2 soot mixture found in the core region is not completed while in the deposition torch flame, and was shown by Li [**7**] to be dependent on the substrate temperature. The GeO_2 structure of the mixture is all crystalline below 400 °C. The GeO_2 soot deposited between 500 and 800 °C has a linearly increasing percentage of non-crystalline forms of GeO_2 mixed with the SiO_2. The non-crystalline forms of GeO_2 have a higher soot density, which causes the axial speed of core soot growth to decrease, given constant mass flowrates of $GeCl_4$ and $SiCl_4$ to the torch. This phenomenon has been observed in experiments that show changes in pull speed corresponding to changes in the core substrate temperature (see Fig. 4). The resulting approximately linear relationship between pull speed and substrate temperature can be utilized to provide a model for a control scheme. The pull speed (core soot axial growth rate) may be changed by the core soot substrate temperature.

When the core and clad axial growth rates are not equal, two situations may occur. First, if the core growth rate is faster than the clad rate, then the core tip length will grow and outrun the clad, causing a tapered effect on the cladding outside diameter (see Fig. 2). As the core moves further away from the cladding deposition location, less heat is transferred from the cladding to the core tip. The lower temperature of the core soot substrate decreases the soot density and causes a faster core growth rate (pull speed) for the core, aggravating the situation.

Another undesirable situation is when the clad growth rate exceeds the core growth rate. When the cladding torch deposits faster than the core torch, it

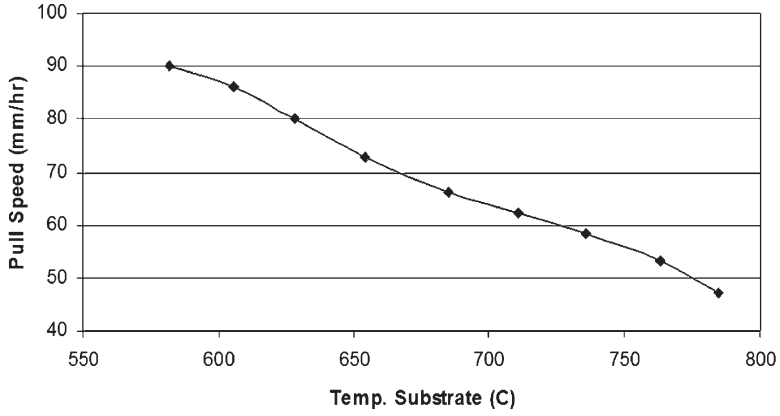

Fig. 4 Experimental data for pull speed (core growth rate) versus soot preform core tip substrate temperature. An approximately linear relationship exists between pull speed and core tip temperature

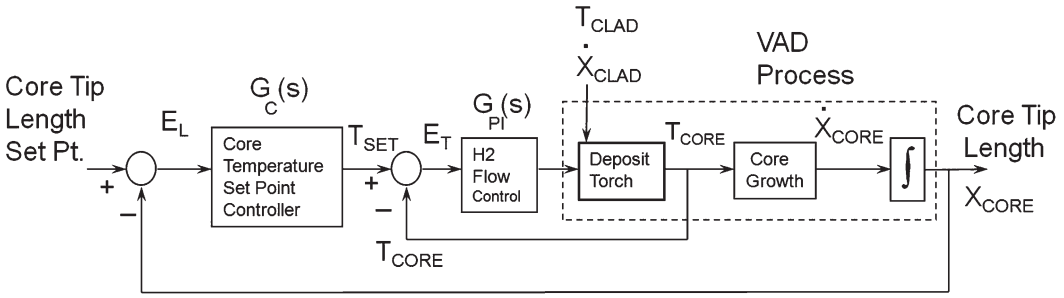

Fig. 5 Proposed VAD cascaded control scheme, with an inner temperature control loop and an outer control for core tip soot, to provide a more uniform final product

causes the cladding surface to engulf the core tip bulging the diameter. As the core tip length is very short in this case, the heat flux from the clad deposition increases as the core deposition surface approaches the core tip. The density of the core soot increases with temperature, causing the core pull speed to continue to slow further. The system can become somewhat unstable.

To address this mismatch of core and clad soot axial growth rates a cascaded controller is proposed to change the core deposition temperature set point in order to correct mismatched growth rates of the core and clad torches. A diagram of the desired cascaded control scheme is given in the functional block diagram of Fig. 5.

3 PROCESS MODEL DEVELOPMENT

3.1 Temperature and deposition modelling and control

In order to gain insight into the process and explore potential controllers, a model of the described VAD process was needed. In this work a VAD core substrate temperature model as a function of H_2 flow to the core torch is

$$\frac{\Delta T_{\mathrm{CORE,H_2}}(s)}{\Delta \mathrm{H_2}(s)} = G_{\mathrm{TEMP}}(s) = \frac{a}{s+b} \quad (^{\circ}\mathrm{C\,min/l}) \tag{2}$$

where $a = 7.51$, $b = 0.0778$, with a PI controller for the H_2 flow, $G_{\mathrm{PI}}(s)$

$$G_{\mathrm{PI}}(s) = K_{\mathrm{p}}\left(s + \frac{K_{\mathrm{i}}}{K_{\mathrm{p}}}\right)\frac{1}{s} \quad (\mathrm{l}/^{\circ}\mathrm{C\,min}) \tag{3}$$

where $K_{\mathrm{i}}/K_{\mathrm{p}} = 0.065$ and $K_{\mathrm{p}} = 0.035$. Equations (2) and (3) were developed in earlier work [**8**], which was employed as part of the system model including deposition rates.

The identified first-order model approximation of the core substrate temperature (T_{CORE}) response to H_2 flow was based on experimental data. This VAD process torch temperature model is expanded here to include the effects of the changing core soot substrate temperature as a function of the core tip length. There are several assumptions made in the development of the core tip length model. The heat fluxes generated from both the clad and core torches are assumed to be constant. This permits modelling of the core substrate temperature as a function of the distance between the heated clad substrate location and the core substrate. As the clad torch gas and chemical flowrates are substantially higher than the core torch (approximately an order of magnitude), the temperature of the clad soot deposition location is treated as unaffected by its proximity to the soot core tip (core deposition location). The core torch has little influence on the clad deposition rate, as can be seen in Fig. 6.

Based on these assumptions a suitable VAD process model can be developed to address core substrate temperature changes and core tip growth. It should be noted that the thermal model presented here is a highly simplistic model without the complex thermal boundary conditions required in a rigorous thermal analysis. The model is designed to provide basic insight into a potential control scheme.

The clad torch produces a relatively constant temperature (T_{CLAD}) and heat flux ($q_{\mathrm{CLAD,SS}}$) per area (A) at the clad soot substrate deposition location. The core substrate temperature, T_{CORE}, thermal conductivity, k_{TH}, and the core substrate tip length, L_{CORE}, are modelled, applying the constant heat flux to the heat conduction equation as follows

$$\frac{q_{\mathrm{CLAD,SS}}}{A} = k_{\mathrm{TH}}\left[\frac{T_{\mathrm{CLAD}} - T_{\mathrm{CORE}}}{L_{\mathrm{CORE}}}\right]_{\mathrm{SS}} \approx \mathrm{constant} = \beta \tag{4}$$

It has been previously shown that T_{CLAD} is a higher value than T_{CORE} [**8**]. The core tip length is variable and is expressed as

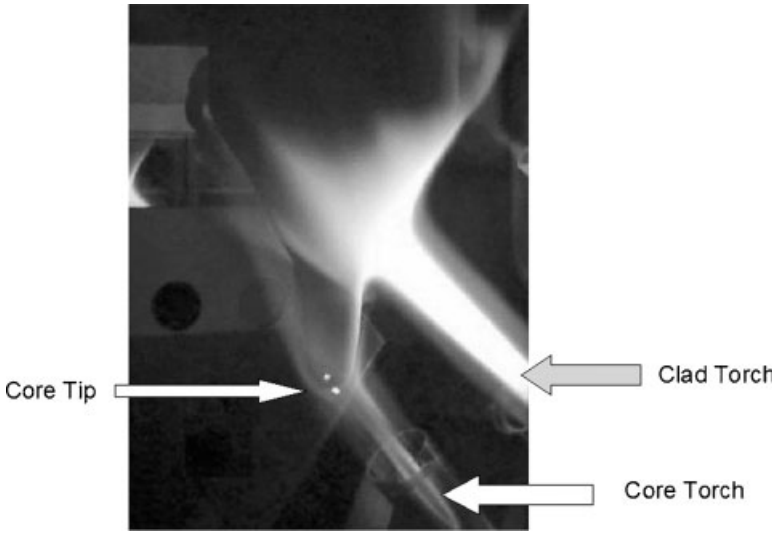

Fig. 6 Typical core and clad deposition in the VAD process

$$L_{\mathrm{CORE}} = L_0 + \Delta L, \qquad L_0 = 50\,\mathrm{mm} \tag{5}$$

$$T_{\mathrm{CORE}} = T_{\mathrm{CLAD}} - \frac{q_{\mathrm{CLAD,SS}}}{A}\left(\frac{L_{\mathrm{CORE}}}{k_{\mathrm{TH}}}\right) \tag{6}$$

Replacing the heat flux per area term in equation (6) using equation (4), the substrate temperature, T_{CORE}, may be rewritten as

$$T_{\mathrm{CORE}} = T_{\mathrm{CLAD}} - \frac{\beta(L_0 + \Delta L)}{k_{\mathrm{TH}}} \tag{7}$$

where β = constant. The core soot substrate temperature, T_{CORE}, may be viewed as the superposition of the initial core temperature, $T_{\mathrm{CORE,0}}$, plus the temperature change caused by the thermal resistance variation, related to core soot tip length, $\Delta T_{\mathrm{CORE\_LENGTH}}$

$$T_{\mathrm{CORE}} = T_{\mathrm{CORE,0}} + \Delta T_{\mathrm{CORE\_LENGTH}} \tag{8}$$

where $T_{\mathrm{CORE,0}} = T_{\mathrm{CLAD}} - \beta L_0 / k_{\mathrm{TH}}$.

The temperature variation term, $\Delta T_{\mathrm{CORE\_LENGTH}}$, is further redefined by separating and equating the variational terms of equations (7) and (8); $\Delta T_{\mathrm{CORE\_LENGTH}}$ is given by the following equation, where k_{TH} is not constant

$$\Delta T_{\mathrm{CORE\_LENGTH}} = \frac{\beta(\Delta L)}{k_{\mathrm{TH}}} \tag{9}$$

The thermal conductivity of SiO_2 is dependent on the soot structure and temperature. For a ceramic structure the thermal conductivity is linear [**9**]. A near-perfect fit of the thermal conductivity versus temperature data yields a linear relation

$$k_{\mathrm{TH}} = 0.83 + (0.00105)T \quad (\mathrm{W/m\,K}) \tag{10}$$

where $T = 0.5(T_{\mathrm{CORE}} + T_{\mathrm{CLAD}})$. Using equations (2) to (10) a simple thermal model can be developed to represent the core substrate temperature as a function of heat flux, clad temperature, core torch H_2 flow, and core length.

3.2 VAD process model diagram

A block diagram of the system model of the soot core and clad temperatures including the core soot axial growth rate, based on the previously discussed assumptions and presented data, is provided in Fig. 7. This is a more detailed VAD process representation of the rightmost three blocks of Fig. 5, accounting for additional system parameters.

A regression (with a square of the sample correlation coefficient, r^2, value of 0.993) of the pull speed versus temperature data of Fig. 4 yields the following relationship for core axial growth rate (pull speed) as a function of time (G_{CORE} in Fig. 7)

$$\dot{X}_{\mathrm{CORE}} = 210.46 - 0.20783 T_{\mathrm{CORE}} \tag{11}$$

In equation (11), the core axial growth rate is expressed in units of mm/h and the unit for temperature is °C.

3.3 Deposition model response: open loop

A computer simulation of the process was created with MATLAB™/Simulink™ (MathWorks, Inc.)

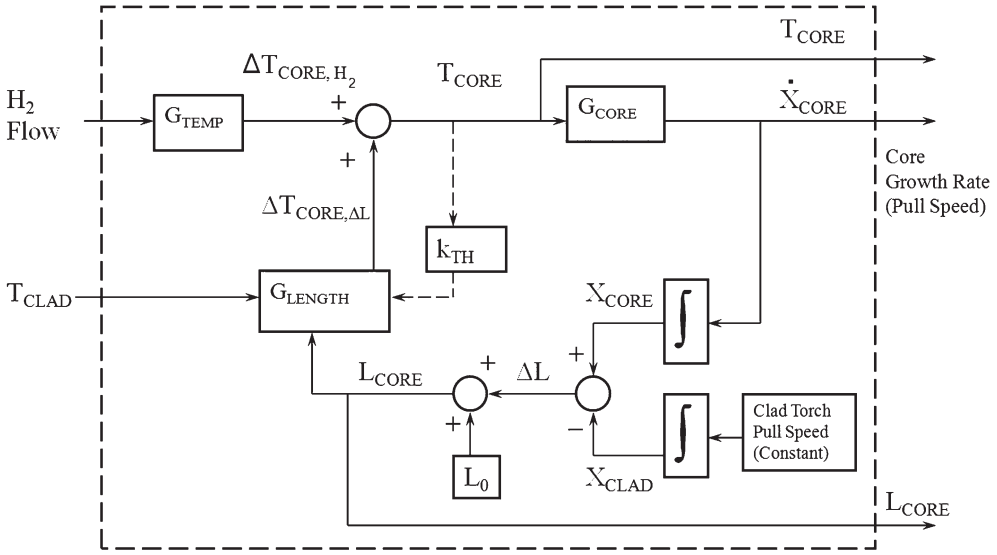

Fig. 7 System model block diagram of the core soot substrate temperature and growth

based on the block diagrams of Figs 5 and 7. The function blocks G_{TEMP}, G_{LENGTH}, and G_{CORE} are derived from equations (2), (9), and (11), respectively.

Axial deposition growth rates (pull speeds) of 50 mm/h or higher are common in industry [**10**]. Simulations performed had intentionally mismatched axial growth rates for the depositions of the clad and core torches (60 and 65 mm/h respectively). The core substrate temperature set point (and initial condition) was 700 °C while the clad substrate temperature was a constant 850 °C. The previously developed temperature controller [**8**] was implemented to regulate the core substrate temperature. However, no control was initially applied to regulate the core tip length, L_{CORE}, representing the original open-loop system. As a result the core tip length grew linearly from 40 to 60 mm over 4 h of deposition, as expected with the 5 mm/h mismatch in clad and core axial deposition rates, and maintained core substrate temperature. Simulation data are shown in Fig. 8.

The starting diameters for the core and clad soot were 40 and 200 mm respectively. With the aforementioned mismatched axial deposition rates, where the length of the core was growing faster than that of the cladding, the resulting outside diameter of the preform would narrow as the core tip lengthened. This is attributable to the constant volumetric flowrates through each deposition torch and a constant core soot diameter

$$Q_{\text{CLAD}} = \frac{\pi}{4}\left(D^2 - d^2\right)\dot{X}_{\text{CORE}} = \text{constant} \tag{12}$$

For this particular geometry and scenario, the outer clad diameter (D) is reduced to 192.5 mm from the original 200 mm. Additional control is required to meet a process specification of 1 per cent variation on the diameter.

4 CORE TIP LENGTH CONTROL DESIGN

To complete the cascaded control design, the outer control loop for core tip length regulation must be established. Although this deposition process is a coupled multiple-input–multiple-output (MIMO) system, the core tip length can be considered primarily a first-order system as a function of time (essentially an integral function), dependent upon the mismatch of the clad and core axial deposition rates. Considering the core tip length as a first-order system, proportional control of sufficiently high gain or a PI (proportional-integral)-type or PID (proportional–integral–derivative)-type controller should be adequate to regulate the system. Other design considerations are the sampled system stability, sensor noise, and allowable tolerance of the diameter deviation.

For the core tip controller, negative gains were required owing to how the core tip length error affects the core tip growth. When the core tip is too long, the core tip length error is negative and reduces the temperature set point. The reduction in temperature decreases soot density and further increases core growth rate, making the situation worse. The correct controller outcome reduces the soot density with an increase in core substrate tempera-

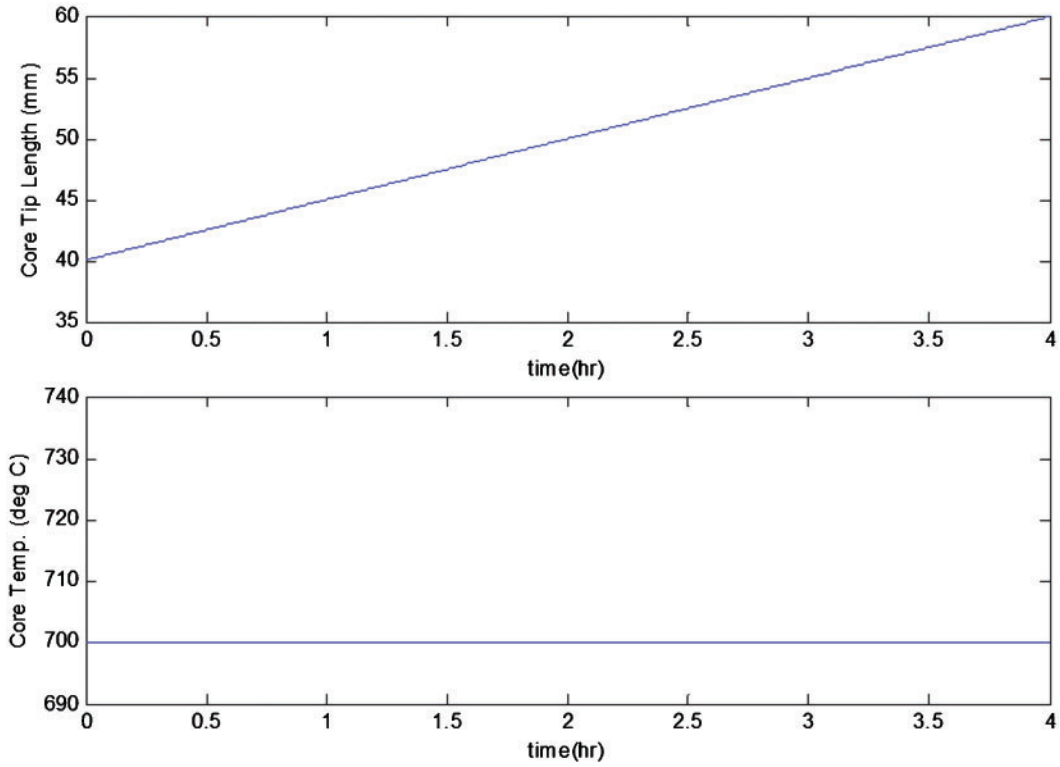

Fig. 8 Open-loop response of the VAD process: core tip temperature (top); core tip substrate temperature (bottom). Mismatched axial deposition rates for the core and clad torches are 65 and 60 mm/h, respectively

ture set point for a negative length error. Likewise, a decrease in the core substrate temperature set point corresponds to a positive length error. Thus, a negative controller gain is required to not create a 'real' positive feedback situation.

An initial core length controller design was based on a discrete root locus of the combined closed-loop temperature control inner loop with the integral function for core tip length. Figure 9 depicts the discrete root locus for the open-loop core tip length transfer function

$$G_{\mathrm{TCORE-CL}}(s)G_{\mathrm{CORE}}(s) = \frac{K_{\mathrm{P}}(0.2631\,s + 0.0171)}{s^3 + 0.3409\,s^2 + 0.0171\,s} \tag{13}$$

which includes the embedded closed-loop temperature control based on equations (2) and (3) as well as system gain, given a sampling interval of 1 s. Using the data from Fig. 9, the limits of the stability require an overall proportional gain of less than 2.23. While a value of 0.099 (or lower) is required for a maximum of 1 per cent overshoot on the core tip length, no overshoot requires $K_{\mathrm{P}} \leqslant 0.073$; thus $K_{\mathrm{P}} = 0.073$ was selected. This value cannot be used directly in the controller, as the overall natural gain of the system (including all conversion factors) without control must be included.

The overall gain of the forward open-loop for the core tip length without any control gain is 1.363×10^{-5}, accounting for all units. This value was divided into the selected proportional gain ($K_{\mathrm{P}} = 0.073$) to yield the correct controller proportional gain of 5355 °C/mm.

While proportional control alone should satisfy the control and process requirements, the addition of integral control can eliminate steady-state error for a set point. The amount of integral control necessary was dependent on the permissible settling for reduction of the error and system stability. Root loci data for stability limits with varying controller pole positions for a PI controller are given in Fig. 10. (Note that the added system zero from the addition of integral control is $K_{\mathrm{i}}/K_{\mathrm{p}}$.) The continuous and discrete equations for the combined system model with the controller are

$$G_{\mathrm{C}}(s)G_{\mathrm{TCORE-CL}}(s)G_{\mathrm{CORE}}(s) = K_{\mathrm{p}}\left(\frac{s + K_{\mathrm{i}}/K_{\mathrm{p}}}{s}\right)\left(\frac{0.2631\,s + 0.0171}{s^3 + 0.3409\,s^2 + 0.0171\,s}\right) \tag{14}$$

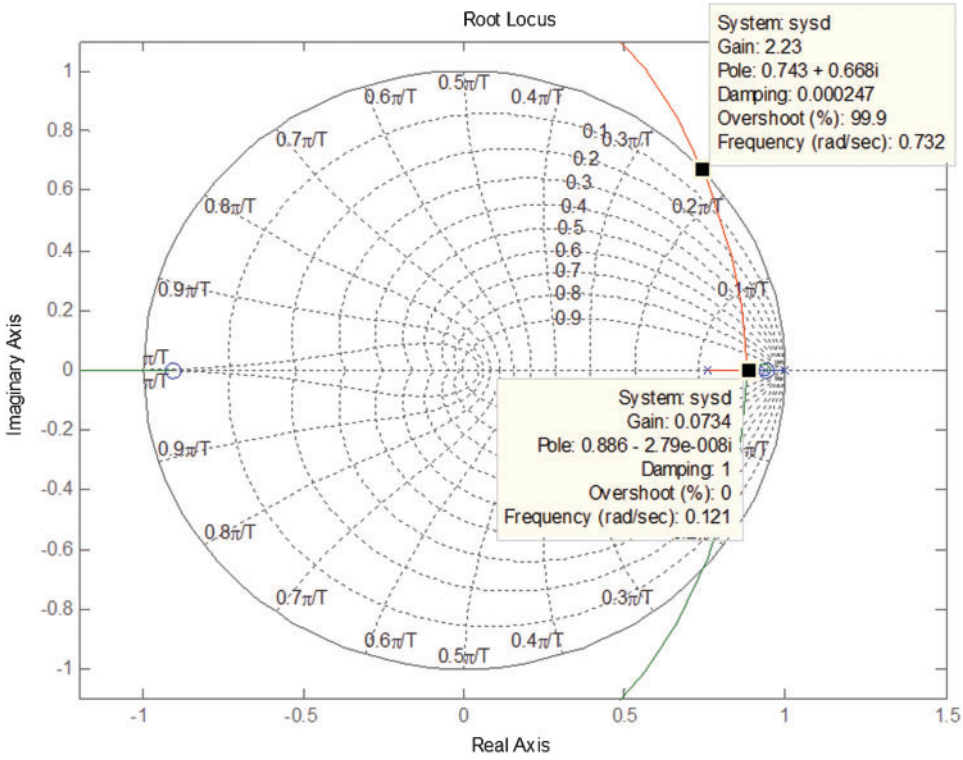

Fig. 9 Discrete domain root locus for the open-loop core tip length transfer function with the embedded temperature control

From Fig. 10 the upper limits on the integral gain can be established at $K_i/K_p = 0.2$. Root loci were examined to determine the PI controller pole, ranging from 0.20 to 0.01 rad/s. For each value the largest damping ratio for the closed-loop dominant pole was determined. Figure 11 shows such a selection. Plotting the damping ratio and dominant discrete closed-loop pole versus the K_i/K_p ratio (Fig. 12) yielded an optimal gain selection of an overall system gain of 0.904 and a K_i/K_p ratio of 0.02.

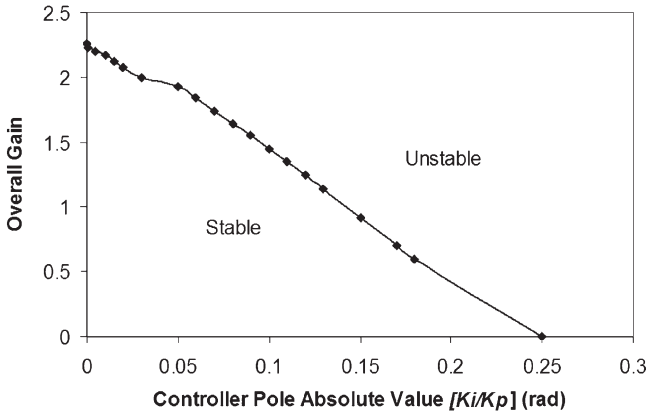

Fig. 10 Stability limits for discrete domain root loci for the open-loop core tip length transfer function with PI controller

With two potential core tip length control schemes defined, simulation studies were conducted to evaluate the efficacy of the approaches.

5 SIMULATION AND RESULTS

Figure 13 presents the simulated closed-loop response for the core tip length and core substrate temperature as functions of time, using the proportional controller designed to regulate the core tip length. There was a small, steady-state error in the core tip length. Results for the established PI controller for the core tip length are provided in Fig. 14. The same mismatched axial growth rates for the clad and core axial depositions (60 and 65 mm/h, respectively) were modelled in all simulations. The process was able to achieve a constant core length after a period of time in both cases. However, the PI controller had no steady-state error.

With increased integrator gain the core tip length error can be brought to zero faster, but with some additional oscillation, in temperature error and core tip length error. The addition of derivative control to the PI controller to create a PID controller offered substantial improvement in system performance to

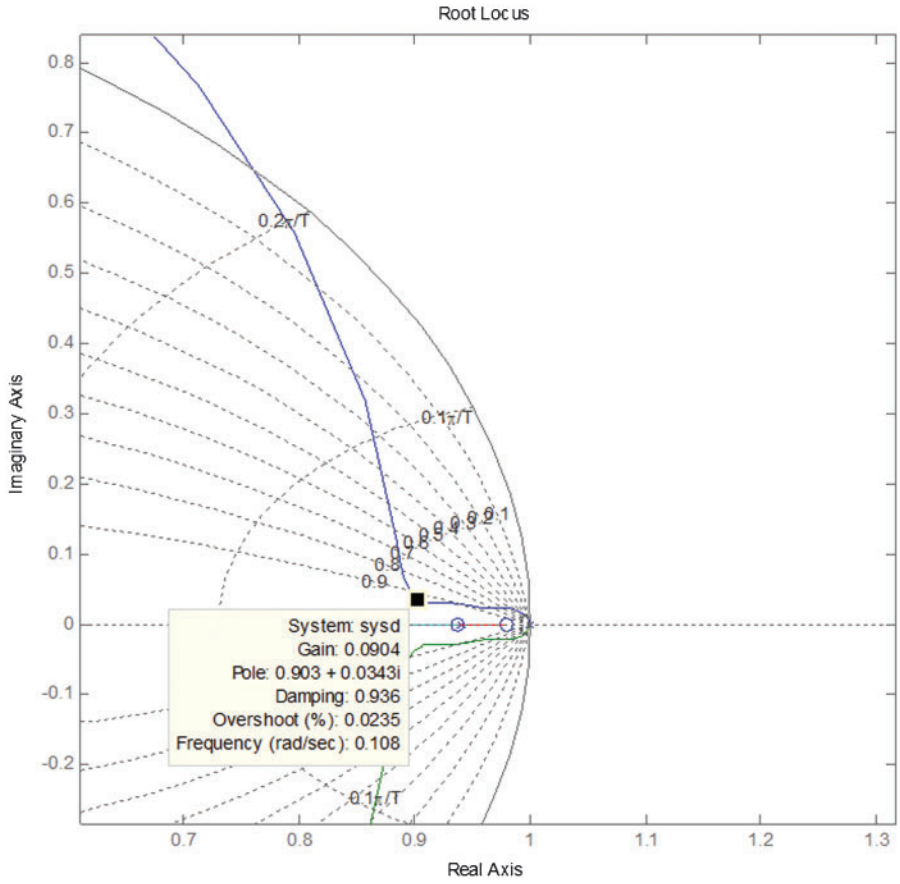

Fig. 11 Discrete domain root locus for the core tip length transfer function with PI controller. Controller pole (K_i/K_p) value is 0.02

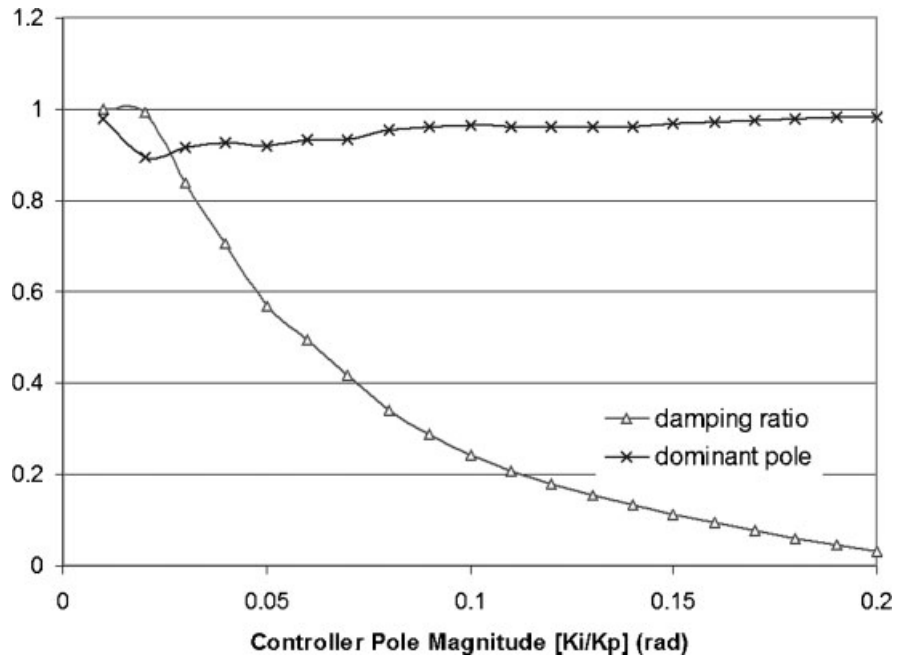

Fig. 12 Damping ratio and dominant system pole for the closed-loop core tip length transfer function with PI controller versus controller pole (K_i/K_p)

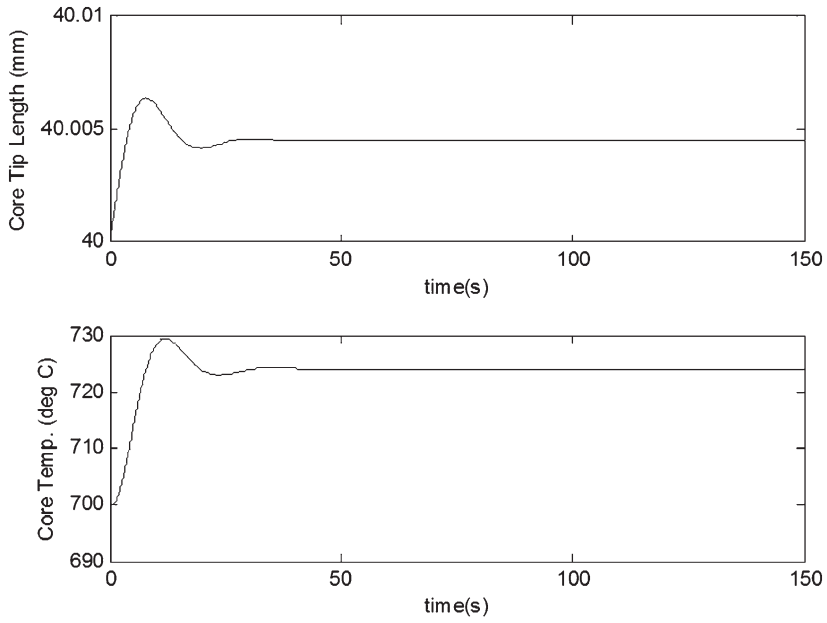

Fig. 13 P control closed-loop response of the VAD process: core tip temperature (top) and core tip substrate temperature (bottom) with a proportional control gain magnitude of 5355 °C/mm (overall system gain of 0.073)

respond quickly and reduce oscillation and overshoot, as seen in Fig. 15.

Modelling of filtered (0.15 Hz) random sensor noise of ± 0.02 mm for the core tip length sensor yields substantial disturbances in the core temperature (see Figs 16, 17, and 18). However, this sensor and temperature disturbance does not translate to significant core length variation. The PI-type control removes the small steady-state error present in the P control. Again the PID-type controller was seen to provide further improvement in the controller's ability to reject noise.

6 CONCLUSION

A closed-loop scheme for cascaded control of the core tip length and core substrate temperature has been modelled and simulated. A marked decrease in

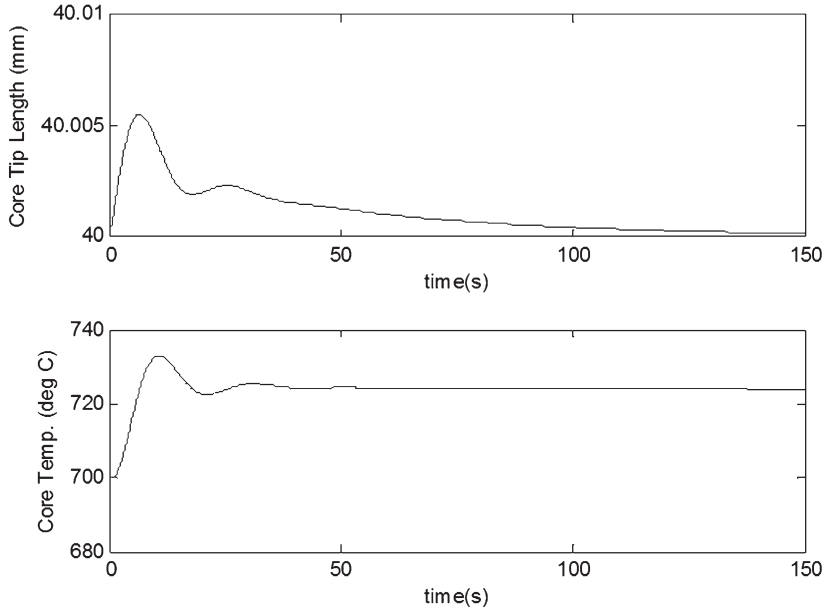

Fig. 14 PI control closed-loop response of the VAD process: core tip temperature (top) and core tip substrate temperature (bottom) for a proportional control gain magnitude of 6630 °C/mm and an integral gain ratio of 0.020 (integral gain of 132.60 °C/mm)

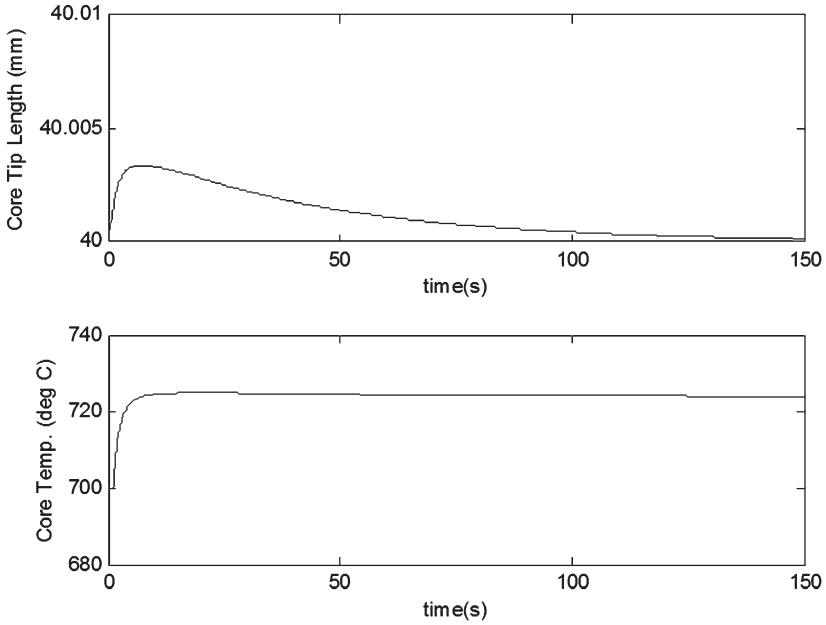

Fig. 15 PID control closed-loop response of the VAD process: core tip temperature (top) and core tip substrate temperature (bottom) for a proportional control gain magnitude of 6630 °C/mm, an integral gain of 132.60 °C/mm, and a derivative gain of 26 520 °C/mm

the potential for mismatch between the core and clad soot deposition rates underlying soot core tip variations is demonstrated by the model. The control of the core tip length forces the deposition rates of the core and clad to be matched. The simulated model results indicate a significant potential improvement in the obtainable geometry of soot preforms. The cascaded controller proposed appears to be relatively uncomplicated to implement.

A comparison of the performance between the proportional and proportional plus integral control has been given with results as expected. It can be

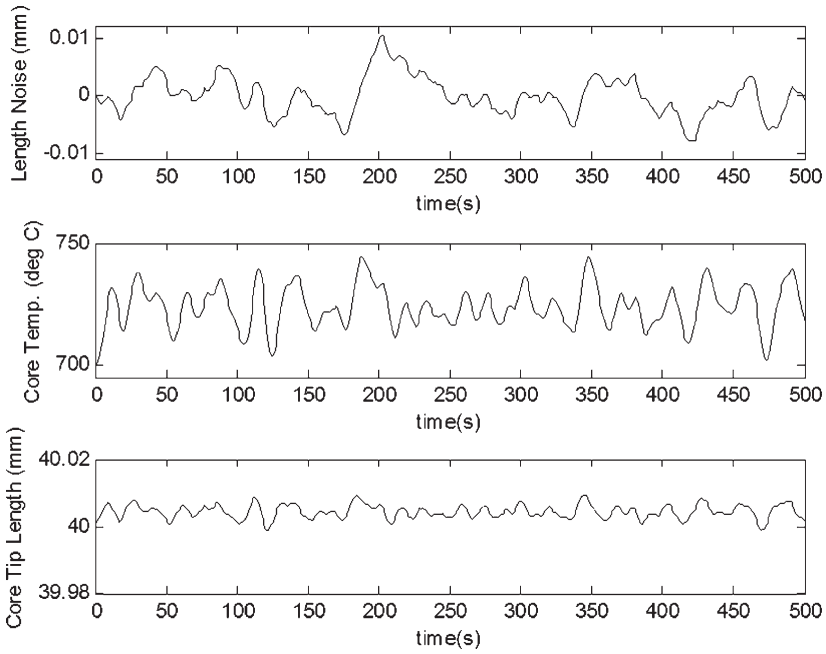

Fig. 16 Simulation of the closed-loop system with sensor noise: sensor noise (top), temperature (middle), core tip length (bottom). Closed-loop response with P control of the core temperature control in the cascaded control scheme

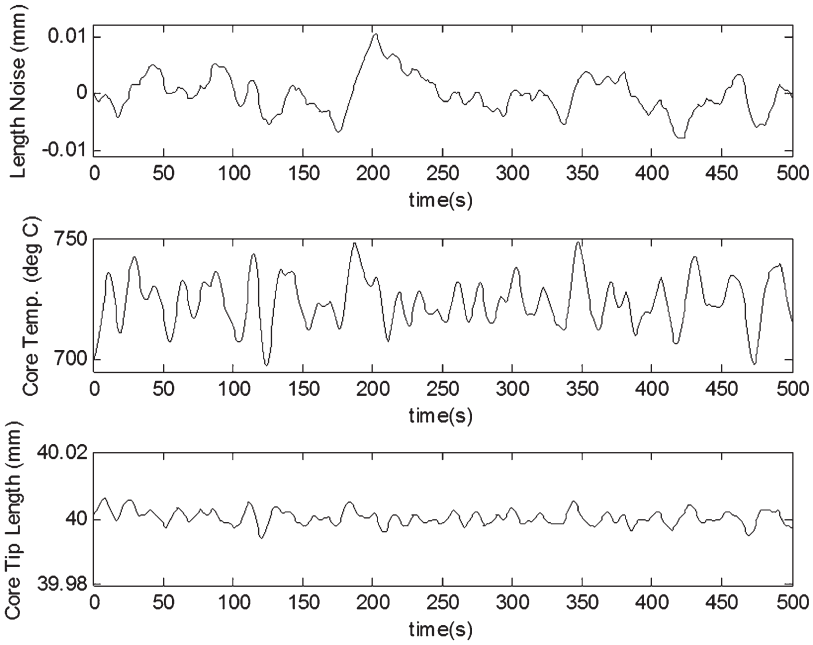

Fig. 17 Simulation of the closed-loop system with sensor noise: sensor noise (top), temperature (middle), core tip length (bottom). Closed-loop response with PI control of the core temperature control in the cascaded control scheme

noted from the results of the PI control that the response to the step changes has slowed; however, the steady state error was removed. No actuator saturation has been observed in the system model. Also, since the time constant of the controlled system is relatively slow, a broad spectrum of controllers would be suitable. A PID controller, adding derivative control to the existing PI controller, was examined; the resulting PID controller improved the speed of the response and noise rejection, compared to the P or PI controller.

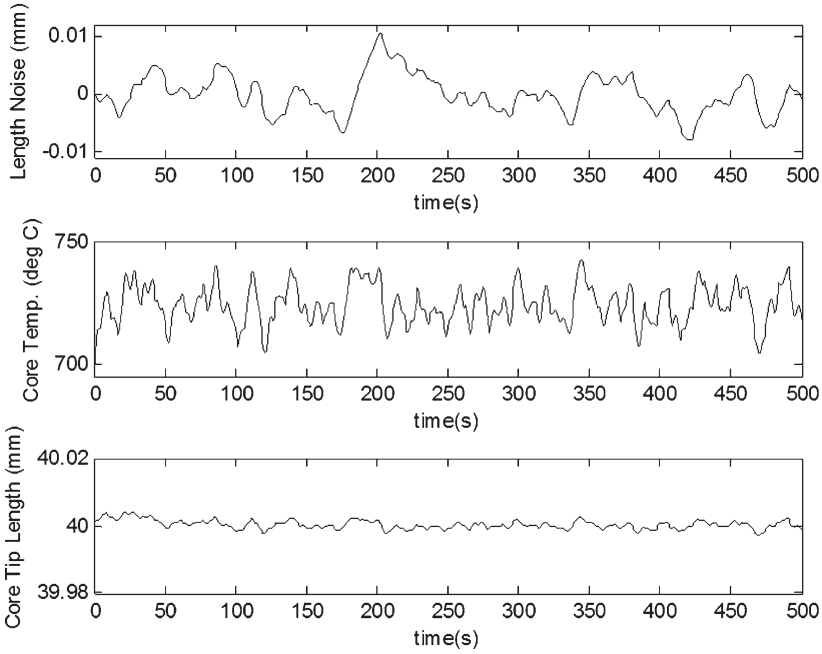

Fig. 18 Simulation of the closed-loop system with sensor noise: sensor noise (top), temperature (middle), core tip length (bottom). Closed-loop response with PID control of the core temperature control in the cascaded control scheme

The achievable system performance of the proposed control scheme may be less than predicted by the model, and will be dependent on sensor noise, unmodelled disturbances, and unmodelled system complexities. Although proportional control or PI-type control of the core length appears adequate, the PID controller offers additional performance advantages. The simulation studies raise further modelling questions, and suggest that actual tests be conducted.

REFERENCES

1 **Izawa, T., Miyashita, T.,** and **Hanawa, F.** *Continuous fabrication of high silica fiber preform*. US Patent 4,062,665, 1977.
2 **Keck, D. B., Schultz, P. C.,** and **Zimar, F.** *Method of forming optical waveguide fibers*. US Patent 3,737,292, 1973.
3 **Refi, J.** *Fiber optic cable: a light guide*, 1991 (ABC Teletraining, Geneva, Illinois).
4 **Choi, M., Park, J. S.,** and **Cho, J.** Modelling of chemical vapour deposition for optical fiber. *Opt. Quantum Electron.*, 1995, **27**(5), 327–335.
5 **MacChesney, J. B., O'Connor, P. B.,** and **Presby, H. M.** A new technique for the preparation of low-loss and graded index optical fibers. *Proc. IEEE*, 1974, **62**(9), 1282–1283.
6 **MacChesney, J. B.** and **DiGiovanni, D. J.** Materials development of optical fiber. *J. Am. Ceram. Soc.*, 1990, **73**(12), 3537.
7 **Li, T.** (Ed.) *Optical fiber communications*, vol. 1, 1985 (Academic Press, Inc., Orlando, Florida).
8 **Jenkins, H. E.** and **Radharamanan, R.** Closed-loop control in the VAD process: a case study for modeling and control. In Proceedings of the International Symposium on *Flexible automation*, Osaka, Japan, 2006.
9 **Shakelford, J. F.** and **Alexander, W.** (Eds) *CRC materials science and engineering handbook*, 2001, p. 284 (CRC Press, Boca Raton, Florida).
10 **Suda, H., Sudo, S.,** and **Nakahara, M.** Fine glass particle-deposition mechanism in the VAD process. *Fiber Integrated Opt.*, 1983, **4**(4), 427–437.

APPENDIX

Notation

A	area, effective heat flow normal area
d	core diameter of preform
D	clad diameter of preform
G_{CORE}	core axial deposition function
G_{LENGTH}	core tip length function
G_{P}	plant transfer function from $H_2(s)$ to $T_{\mathrm{CORE}}(s)$
G_{PI}	PI controller transfer function T_{CORE}
G_{TEMP}	core temperature function
k_{TH}	thermal conductivity
K_{i}	integral gain
K_{p}	proportional gain
L_{CORE}	length of core soot tip
L_0	initial length of core substrate soot tip
PI	proportional-integral control
Pull speed	rate of preform deposition axial growth
$q_{\mathrm{CLAD,SS}}$	heat flow from clad substrate
Q_{CLAD}	volumetric deposition rate of clad torch
$T_{\mathrm{CORE},0}$	core soot substrate temperature initial
T_{CORE}	core soot substrate temperature
T_{CLAD}	clad soot substrate temperature
VAD	vapour-phase axial deposition
$\dot{X}_{\mathrm{CORE}}$	core soot axial growth rate, or pull speed
$\dot{X}_{\mathrm{CLAD}}$	clad soot axial growth rate
β	heat flux (constant)
$\Delta H_2(s)$	hydrogen flowrate change to core torch
ΔL	change in length of core soot section
$\Delta T_{\mathrm{CORE\_LENGTH}}$	core substrate temperature change from core tip length change